

Ultrafast Intersubband Relaxation in SiGe Quantum Well Structures

P. Rauter¹, T. Fromherz¹, N.Q. Vinh², B.N. Murdin³, J.P. Phillips²,
C.R. Pidgeon⁴, L. Diehl⁵, G. Dehlinger⁵, D. Grützmacher⁵, Ming Zhao⁶,
Wei-Xin Ni⁶, G. Bauer¹

¹ Institute for Semiconductor and Solid State Physics, University Linz,
Austria

² FOM Institute for Plasma Physics Rijnhuizen, Nieuwegein, Netherlands

³ University of Surrey, University Linz, Austria

⁴ Heriot-Watt University, Edinburgh, UK

⁵ Paul Scherrer Institut, Villingen, Switzerland

⁶ University of Linköping, Linköping, Sweden

We report the quantitative and direct determination of hole intersubband relaxation times in a voltage biased SiGe heterostructure using density matrix calculations applied to a four-level system in order to interpret photocurrent pump-pump experiments. One consistent set of parameters allows the simulation of two kinds of experiments, namely pump-pump photocurrent experiments at a free electron laser (wavelength 7.9 μm) and the laser-power dependence of the photocurrent signal. This strongly confirms the high reliability of these parameter values, of which the most interesting in respect to Si based quantum cascade laser development is the extracted heavy-hole relaxation time. The simulations show that this relaxation time directly determines the experimentally observed decay of the pump-pump photocurrent signal as a function of the delay time. For a heavy hole intersubband spacing of 160 meV, a value of 550 fs was obtained. The experimental method was further applied to determine the LH1-HH1 relaxation time of a second sample with a transition energy below the optical phonon energy. The observed relaxation time of 16 ps is consistent with the value found for the same structure by transmission pump-probe experiments.

Introduction

The strong need for cheap and integrable Si-based optoelectronic devices for a wide range of applications has been inducing considerable endeavor to develop structures for light emission, modulation and detection in this material system. While recent breakthroughs bring the concept of transition from electrical to optical interconnects closer to realization, the base for any silicon photonics, namely a group IV laser source, still waits to be developed. Up to now, the only lasing device demonstrated in Si is a Raman laser [2], which essentially lacks the advantages associated with the silicon system by requiring an external pump laser source. For silicon as an indirect semiconductor the concept of infrared emitters based on quantum cascade (QC) heterostructures, which is very successfully applied to III-V material systems, provides a promising approach towards a SiGe infrared laser. But despite the successful demonstration of infrared electroluminescence (EL) of various wavelengths for p-type SiGe quantum cascade structures, lasing has yet to be achieved. The build-up of population inversion in order to achieve lasing fundamentally depends on the relaxation lifetime of the excited energy level of the lasing transition. Therefore the measurement and optimization of

the intersubband relaxation time constitutes a key issue for the realization of a Si cascade laser source. The intersubband hole relaxation time for transitions *below* the optical phonon energy (Si–Si: 58 meV, Ge–Ge: 36 meV) is significantly larger than 10 ps and therefore is experimentally well accessible [3]. The lifetimes for energies *above* the optical phonon energies are smaller than 1 ps and are limited by optical deformation potential scattering [4]. So far experiments aimed at the measurement of the lifetime of hole intersubband transitions in this energy range suffered from a lack of time resolution [5] or from hole heating requiring subtraction of heating contributions in order to gain a value for the relaxation time [4].

Results and Discussion

Two samples are investigated in this work. Sample 1 for time resolved measurements at transition energies higher than the optical phonon energy was grown pseudomorphically on a Si [100] substrate at low nominal temperature (350 °C). The active region consists of five $\text{Si}_{1-x}\text{Ge}_x$ valence band QW (widths: 39, 26, 24, 23 and 35 Å; Ge content: 0.42, 0.42, 0.40, 0.37, and 0.28 respectively) and is *p*-type doped ($5 \times 10^{17} \text{ cm}^{-3}$). This sequence is repeated ten times and separated by an undoped 500 Å Si barrier. The ten QW periods were sandwiched between 300 nm (100 nm) *p*-type ($2 \times 10^{18} \text{ cm}^{-3}$) bottom (top) contacts. The structure was processed into mesa stripes of $7 \times 0.5 \text{ mm}$ and contacted with an Al:Si metallization in order to measure the vertical PC. On samples containing similar sets of undoped QW with only a thin barrier between the QW series, QC EL has been observed [6]. Self consistent *k*.*p* bandstructure calculations have been performed, providing the dipole matrix elements required for the density matrix simulations. The HH1–HH2 transition energy of the deepest well 1 (39 Å, 42 % Ge) is calculated to be 160 meV. Sample 2 with transition energies below the optical phonon energy was grown by MBE on 30% Ge pseudosubstrate. One period of the active region consists of one $\text{Si}_{0.67}\text{Ge}_{0.33}$ valence band QW with a width of 50 Å and two 16 Å wide $\text{Si}_{0.8}\text{Ge}_{0.2}$ barriers flanking the well. This *p*-type doped ($1 \times 10^{18} \text{ cm}^{-3}$) sequence is repeated 12 times and separated by undoped 100 Å Si barriers. The 12 QW periods were sandwiched between 300 nm (100 nm) *p*-type ($2 \times 10^{18} \text{ cm}^{-3}$) bottom (top) contacts. Sample 2 was processed analogue to sample 1. The HH1–LH1 transition energy is calculated to be 32 meV. For this sample, pump-probe transmission experiments revealed an HH1–LH1 lifetime of 20 ps [7]. The height of the PC peak induced by a free electron laser (FEL) pulse was measured as a function of the FEL micropulse energy for TM polarized radiation in order to verify that a nonlinear absorption process is responsible for the PC signal at the HH1–HH2 energy. For pulse energies smaller than $3 \times 10^{-2} \mu\text{J}$ the data presented in Fig. 1(d) show a clear superlinear dependence of the peak maximum on the pulse energy, which is typical for multi-photon processes. A saturation of the PC signal is observed for pulse energies higher than $5 \times 10^{-2} \mu\text{J}$. In order to understand the power dependence of the PC signal over the whole range of micropulse energies as well as the dynamics of the state occupancies, the response of the system to a laser pulse resonant with the HH1–HH2 transition was simulated using a density matrix (DM) approach. The processes and states included in this model are depicted in the inset of Fig. 1(d). The HH1 and HH2 states are labeled by 0 and 1, respectively. The continuum is modeled by two states (2, 3) only. State 2 represents the continuum state that is resonantly coupled to the HH2 state by the radiation field. The relaxation from state 2 into state 3 accounts for the decay from the resonant continuum state into delocalized continuum states not coupled to the QW states by the radiation field but contributing to the measured current. In order to determine the intersubband relaxation times in our samples, the FEL wavelength was tuned into resonance with the targeted transition. Time resolved measurements were performed using the free electron laser (FEL) FELIX at FOM Rijnhuizen. FELIX provides micropulses with full widths at half maximum (FWHM) down to 280 fs and peak powers of 100 MW. The micropulse

repetition rate is 25 MHz, 5 macropulses of 7 μs duration are provided per second. The FEL pulses were split into two, where one of the pulses was delayed passing a movable mirror. The polarization of the undelayed pulse was rotated by 90° into TM. Before coupling into the sample in waveguide geometry, the pulses were made collinear again. The photocurrent through the samples was measured as a function of the pulse delay. Figure 2 compares the experimental results with the simulation. The black (a) and red (b) curves present the PC signals after subtracting a background corresponding to large delays. The green line represents the density matrix simulation results. In the simulations, the HH2–HH1 relaxation time τ_{10} was used as a fitting parameter. With $\tau_{10} = 550$ fs an excellent agreement between measured and simulated results was obtained. Moreover, with this value for τ_{10} also the power dependence of the PC can be accurately modeled over 3 decades of micropulse powers (see Fig. 1(d)). This finding strongly suggests that all relevant processes are included in the simulation and that the extraction of the parameters, most interestingly the HH intersubband relaxation time, is performed correctly. The interpretation of the experimental data is based on the picture presented in Fig. 1. The strong asymmetry of the curves in Fig. 2(a) with respect to the sign of the delay is due to the strong polarization dependence of the transition involved. Negative delays in Fig. 2(a) present results for cases, in which the TM polarized pulse is the first to interact with the sample.

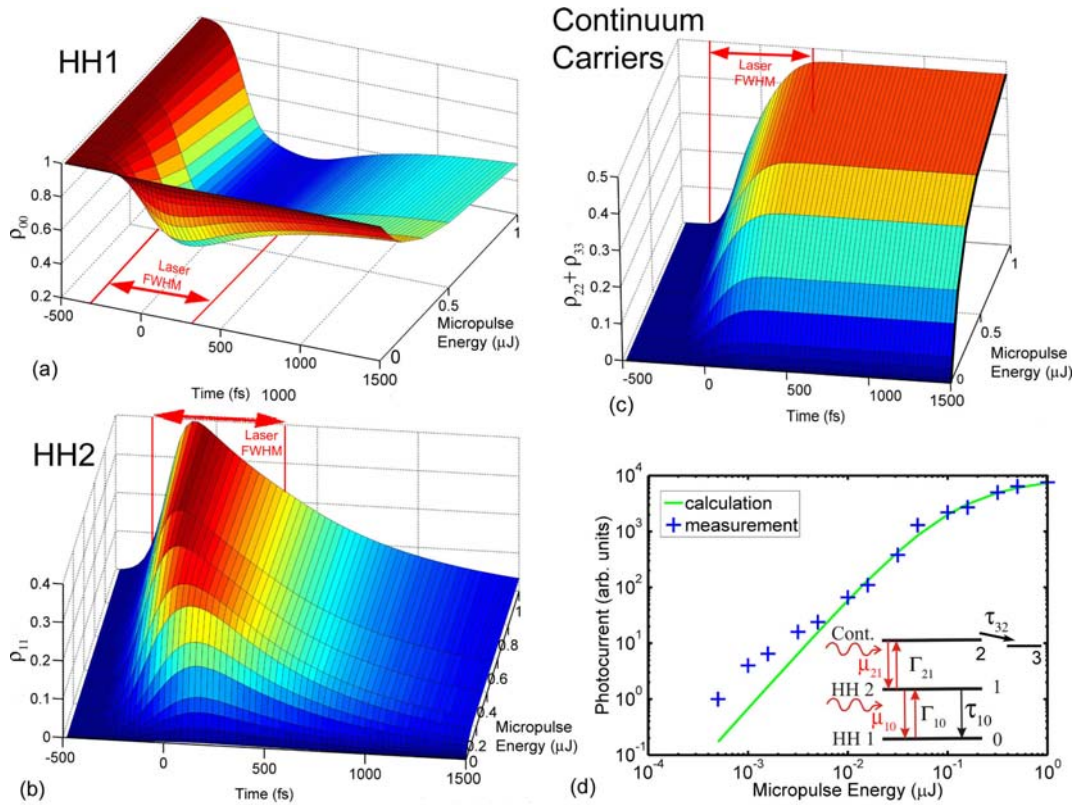


Fig. 1: Sample 1: FEL power dependence of the PC signal. Panel (d) shows a double logarithmic plot of the PC signal vs. the macropulse power of FELIX. The experimental data (crosses) were measured at a bias of 3 V and a temperature of 10 K in TM polarization. The inset sketches the processes considered in the DM calculations, while the plots (a), (b) and (c) show the calculated time evolution of the HH1, HH2 and continuum state occupancies for a TM polarized laser pulse hitting the sample at $t = 0$. The calculated dependence of the PC is shown as solid line in plot (d) and is proportional to the number of continuum carriers at the end of the laser pulse as shown in (c).

In TM polarization the HH1–HH2 transition is allowed, and thus a non-equilibrium population of the HH2 state will build up. This non equilibrium HH2 occupation decays exponentially with the time constant τ_{10} , as presented in Fig. 1(b). From the HH2 state, holes can be excited to the continuum also in TE polarization. Therefore, if the TE pulse hits the structure before the HH2 carriers have relaxed, the integral PC increases proportionally to the residual holes in the HH2 state. Thus the measured decay of the integral PC change as a function of the pulse delay directly monitors the HH2 lifetime, allowing the extraction of the HH2–HH1 relaxation time by performing an exponential fit for the data in Fig. 2(a) gained at negative delays. In TE polarization, HH1–HH2 transitions are forbidden at the Γ point and become only weakly allowed for HH1 vectors with finite momentum perpendicular to the growth direction. Thus only negligible HH2 populations can be excited from the HH1 ground state by a TE pulse. As a consequence, the HH2 relaxation cannot be observed if the TE pulse arrives first (positive delays in Fig. 2(a)), resulting in an asymmetry with respect to the pulse order as observed in the experiment. The fast decaying increase of the PC signal between 0 and 1.5 ps in Fig. 2(a) results from the overlap of the TE and TM pulse, and thus indicates the time-resolution of the experimental setup. The extracted HH2–HH1 relaxation time of 550 fs is significantly longer than the time resolution of the measurement setup. To further confirm experimentally that PC pump-pump experiments probe the excited state lifetime, we compare time resolved pump-pump measurements on sample 2, for which a HH1–LH1 transition time of 20 ps was reported in [7], with conventional pump-probe experiments in transmission. Figure 2(b) shows the result of PC pump-pump measurements at a FEL wavelength of 37.9 μm , a macropulse energy of 70 μJ and an attenuation of 13 dB (red line), where the FEL beams hit the sample surface normally (both beams TE polarized, but cross-polarized). The side peaks found in the experimental data at 15 ps originate from the overlap of the second beam with the fraction of the first beam reflected by the sample’s back surface. The 15 ps delay are consistent with the sample thickness of 600 μm . The reflection of the first pulse is included in the fit presented in Fig. 2(b), which reveals a HH1–LH1 relaxation time of 16 ps in good agreement with the value of 20 ps in [7].

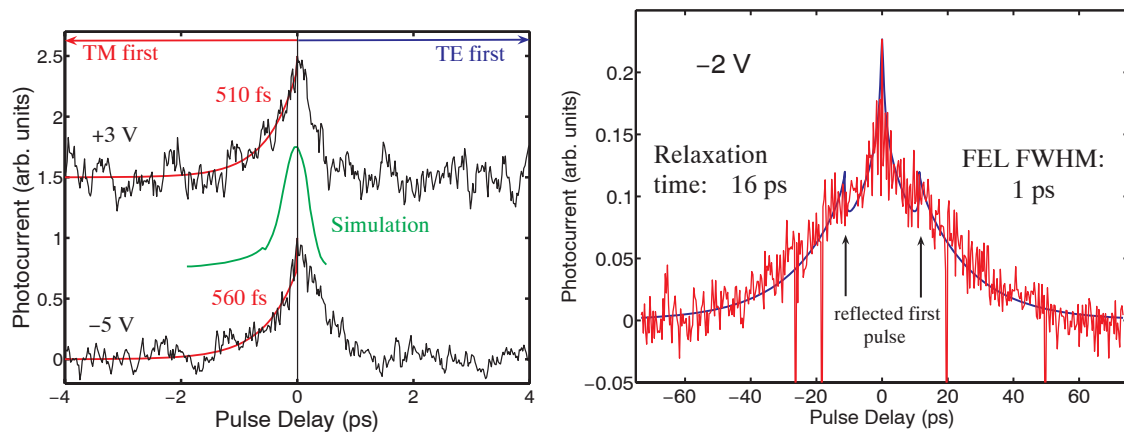


Fig. 2: Plot of the PC as a function of the delay between the TM and TE pump pulses for different bias voltages. A constant background equivalent to the current-integral over the two non-interacting pulses has been subtracted and the traces have been offset vertically for clarity. Sample 1 (a): An exponential fit results in an HH2–HH1 relaxation time of 510 fs for +3 V and 560 fs for -5 V (red lines). Sample 2 (b): The exponential fit of the decay reveals an LH1–HH1 relaxation time of 16 ps (blue line), where the FEL pulse FWHM is 1 ps.

Acknowledgements

This work was supported by the FWF (SFB IRON, Proj. Nrs. F2512-N08, F2507-N08).

References

- [1] A. Liu *et al.*, Nature 427, 615 (2004)
- [2] O. Boyraz *et al.*, Optics Express 12, 5269 (2004)
- [3] R. Kelsall *et al.*, Phys. Rev. B 71, 115326 (2005)
- [4] R. Kaindl *et al.*, Phys. Rev. Lett. 86, 1122 (2001)
- [5] P. Boucaud *et al.*, Appl. Phys. Lett., 69, 3069 (1996)
- [6] G. Dehlinger *et al.*, Science 290, 2277 (2000)
- [7] C. Pidgeon *et al.*, Semicond. Sci. Technol. 20, L50 (2005)